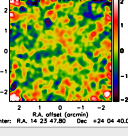


# Public Release of NIKA Sunyaev-Zel'dovich Data

NIKA was used to image galaxy clusters using the Sunyaev-Zel'dovich (SZ) effect. A total of six clusters were observed, providing a pilot project to prepare future NIKA2 observations that are now undergoing at the IRAM 30m telescope.

This web page aims at describing the content of the released data products associated with this project. In case you use it in a publication or in a conference, we ask you to cite at least the main paper corresponding to the respective cluster. While NIKA was a dual band instrument observing simultaneously at 150 and 260 GHz, only the 150 GHz data are released for the time being.

## Data:

Cluster	Redshift	R.A.	Dec.	Image	1 noise realization	Point source model	Data	Main reference
RX J1347.5-1145	0.452	13.0,47.0,30.575	-11.0,45.0,10.08	Small image + clickable link to get a larger one	Small image + clickable link to get a larger one	Small image + clickable link to get a larger one	Only map and point source for this cluster	R. Adam, B. Comis, J. F. Macías-Pérez et al. (2014), A&A 569, A66, arXiv:1310.6237
MACS J1423.8+2404	0.545	14.0,23.0,47.908	+24.0,04.0,42.69				Link to the tar file: map, noise realizations, point source model, transfer function, beam, bandpass	R. Adam, B. Comis, I. Bartalucci et al. (2016), A&A 586, A122, arXiv:1510.06674
MACS J0717.5+3745	0.546	07.0,17.0,31.740	+37.0,45.0,30.73				Link to the tar file: map, noise realizations, point source model, transfer function, beam, bandpass	- R. Adam, I. Bartalucci, G.W. Pratt et al. (2017), A&A 598, A115, arXiv:1606.07721 - R. Adam, M. Arnaud, I. Bartalucci et al. (2016), A&A 606, A64, arXiv:1706.10230
MACS J0717.5+3745 (kSZ model subtracted)	0.546	07.0,17.0,31.740	+37.0,45.0,30.73				Link to the tar file: map, noise realizations, point source model, transfer function, beam, bandpass	R. Adam, I. Bartalucci, G.W. Pratt et al. (2017), A&A 598, A115, arXiv:1606.07721
PSZ1 G046.13+30.75	0.569	17.0,17.0,05.780	+24.0,04.0,26.00				Link to the tar file: map, noise realizations, point source model, transfer function, beam, bandpass	-
PSZ1 G045.85+57.71	0.611	15.0,18.0,20.811	+29.0,27.0,39.10				Link to the tar file: map, noise realizations, point source model, transfer function, beam, bandpass	F. Ruppin, R. Adam, B. Comis et al. (2017), A&A 597, A110, arXiv:1607.07679
CL J1226.9+3332	0.888	12.0,26.0,58.454	+33.0,32.0,48.36				Link to the tar file: map, noise realizations, point source model, transfer function, beam, bandpass	- R. Adam, B. Comis, J. F. Macías-Pérez et al. (2015), A&A 576, A12, arXiv:1410.2808 - C. Romero, M. McWilliam, J. F. Macías-Pérez, et al. (2017), submitted to A&A, arXiv:1707.06113

## **Explanatory supplement:**

### **===== 150 GHz Maps**

The NIKA maps are computed from raw time ordered data using the NIKA processing pipeline. See Catalano et al (2014), Adam et al (2014) and Adam et al (2015) for the main steps of the data reduction. The maps are given in units of surface brightness (mJy/beam). The data are projected on 151x151 pixels grids, where the size of the pixels are 2x2 arcsec. Images include standard astrometric metadata in the header.

### **===== Best-fit Point Source Model**

The NIKA cluster fields contain non negligible radio and sub-millimeter sources identified either from NIKA data themselves, from the literature, or from Herschel data. For each cluster, we provide a point source model extracted from jointly fitting NIKA with higher (Herschel) and lower (literature) frequency data. See Adam et al. (2016) for the procedure. We stress that the flux of each source in the correction maps are not necessarily well constrained, depending on the available external dataset. In addition, it depends on the underlying model that we assume for the SED of each object (either grey body or power law for infrared and radio sources, respectively). Therefore, we recommend to use this model only to quantify the impact of contaminant galaxies, but not to take it as the true contaminant signal.

### **===== Transfer function**

Because of the scanning strategy and the necessary processing to subtract the correlated noise from the time ordered data, the NIKA maps are affected by filtering. This is true in particular for scales beyond the size of the field of view ( $\sim 2$  arcmin).

The amount of filtering is estimated as described in Adam et al. (2015). In brief, we compare the power spectrum of the map of simulated data before and after processing them through the NIKA pipeline. We provide the azimuthally averaged transfer function, as a function of wave number, for each cluster. We note that NIKA data are not sensitive to the zero level surface brightness of the sky. Therefore, the transfer function at wavenumber  $k=0$  is equal to 0. The error bars provide the dispersion of the transfer function measured on individual scans, and thus, are sensitive to variation of atmospheric conditions during the data acquisition. See figure below for an example of the transfer function.

We also provide the following IDL script to be used in order to apply the transfer function to non filtered data, to account for the effects of the reduction. This is to make sure that the definition of the angular frequency,  $k$ , is the same when computing and applying the transfer function onto maps. The raw NIKA maps can also be deconvolved in a similar way but the noise (in particular on the edge of the map) will drastically increase.

---

```
;;----- Inputs
reso: the resolution of the map in arcsec
map_in: the input unfiltered map
Npix: size of the map in pixel (assumes a squared map here)

;;----- Read the transfer functions
tf = mrdfits(your_transfer_function_file, 1, head, /silent)
```

```

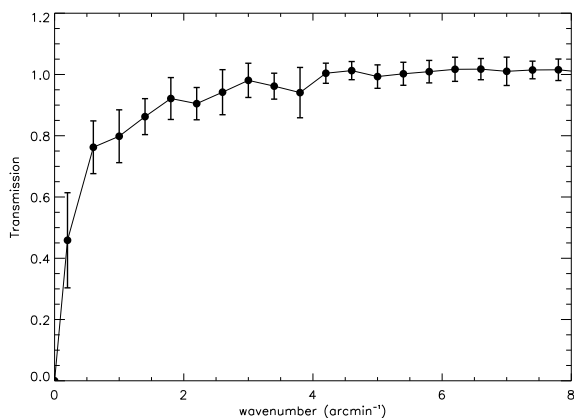
;;----- Get a wave number array
kmax = 1.0/reso
karr = dist(Npix, Npix)
karr = karr/max(karr)*max(kmax)

;;----- Get filtering mapping by interpolating the transfer
function
karr_lin = reform(karr, Npix*Npix)
filtering = interp(tf.tf, tf.wave_number_arcsec, karr_lin)
filtering = reform(filtering, Npix, Npix)

;;----- Apply the filtering
FT_map_in = FFT(map_in)
map_out = double(FFT(FT_map_in * filtering, /inverse))

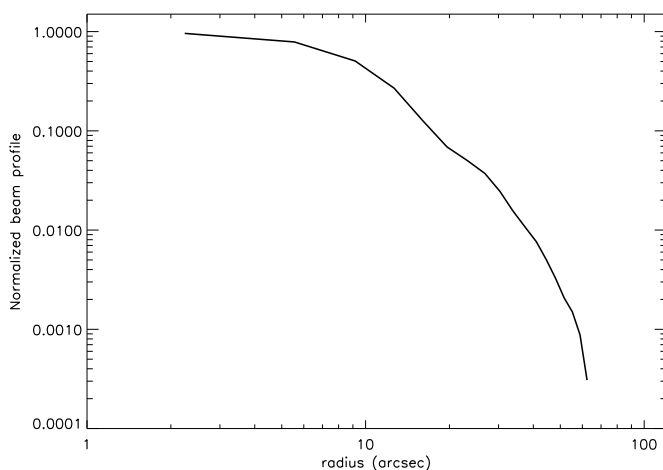
```

---



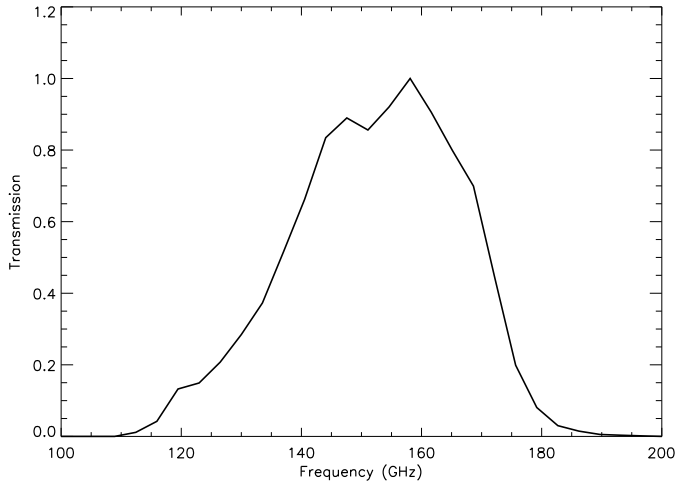
## ===== Beam

The beam profile corresponds to the surface brightness profile of Uranus, normalized by the amplitude of the gaussian best fit of the corresponding map (see figure below). The angular size of Uranus is typically about 3.5 arcsec, and it is neglected as it broadens the main beam by only about 0.7%.



## ===== Bandpass and Unit conversion

We provide the NIKA transmission as a function of frequency, obtained in the case of diffuse emission. See Figure below.



The following tables provide the conversion from Jy/beam to Compton parameter for different gas temperature (see Adam et al. 2017 for more details).

$T_e$ (keV)	$I_0 f(260 \text{ GHz})$	$I_0 f(150 \text{ GHz})$	$I_0 g(260 \text{ GHz})$	$I_0 g(150 \text{ GHz})$
1	3.76	-11.63	7.47	12.40
5	3.31	-11.34	7.30	12.03
10	2.83	-11.00	7.11	11.62
15	2.43	-10.71	6.94	11.24
20	2.06	-10.38	6.81	10.90
25	1.76	-10.17	6.75	10.58

We also provide color correction for typical SED, both for extended emission and point sources. The assumed spectra follow  $f(\nu) \propto \nu^\alpha$ .

$\alpha$	150 GHz				260 GHz			
	Point source		Diffuse source		Point source		Diffuse source	
	p.w.v = 2 mm	5 mm	2 mm	5 mm	2 mm	5 mm	2 mm	5 mm
-3	0.94	0.92	0.99	0.97	0.80	0.78	0.85	0.83
-2	0.97	0.95	1.00	0.98	0.85	0.84	0.89	0.88
-1	0.99	0.98	1.00	0.99	0.90	0.89	0.92	0.91
0	1.00	0.99	1.00	0.99	0.95	0.94	0.95	0.94
1	1.00	1.00	0.99	0.98	0.98	0.98	0.96	0.96
2	1.00	1.00	0.97	0.97	1.01	1.01	0.97	0.98
3	0.98	0.99	0.94	0.95	1.03	1.04	0.98	0.98
4	0.96	0.98	0.91	0.92	1.04	1.05	0.97	0.98

## ===== Noise

For each cluster, we provide a set of 100 noise realizations obtained as described in Adam et al (2016). They include correlated noise as modeled from half difference maps (Jack-Knife), as well as inhomogeneities of the noise due to the scanning strategy. The noise realizations also include the expected contribution from the CIB modeled as described in Adam et al (2017). The latter is largely subdominant for most of the data at 150 GHz, except for the deepest observations of MACS J0717.5+3745 where it becomes significant. The noise contained in the NIKA maps is well described by a gaussian noise, but we stress that it is correlated across pixels of the maps. Therefore, averaging the values of nearby pixels (e.g. when smoothing) does not reduce the noise by  $\sqrt{N}$ .

## ===== Special case of RX J1347.5-1145

The NIKA data provided in this page have been obtained with the final NIKA setup, and are homogeneous, except in the case of the cluster RX J1347.5-1145. For this cluster, the detectors, the optics, the bandpasses and the beam were significantly different (see Adam et al 2014). In addition, the scanning strategy was not optimal due to a mistake in the telescope control system. Therefore, the full characterization of the data was not done for RX J1347.5-1145 and we only provide the raw map in the case of this cluster. We highly encourage to use the data only in a qualitative way (e.g., overlapping contours).

## ===== Special case of MACS J0717.5+3745

The cluster MACS J0717.5+3745 is known to host a significant amount of kinetic SZ signal (Mroczkowski et al. 2012, Sayers et al. 2013, Adam et al. 2017). Therefore, we also provide a map corrected from the best fit kSZ model obtained in Adam et al. (2017). However, we stress that this models remains poorly constrained and is affected by large degeneracies between the cluster gas line-of-sight velocity and the optical depth. Therefore, in the context of thermal SZ studies, we encourage to use the kSZ corrected map to test the stability of any results, with respect to the kSZ contamination, but not to take the kSZ corrected map as the truth.

## Relevant publications:

- R. Adam, O. Hahn, F. Ruppin et al. (2017), submitted to A&A  
Sub-structure and merger detection in resolved NIKA Sunyaev-Zel'dovich images of distant clusters
- C. Romero, M. McWilliam, J. F. Macías-Pérez et al. (2017), submitted to A&A, arXiv:1707.06113  
A multi-instrument non-parametric reconstruction of the electron pressure profile in the galaxy cluster CLJ1226.9+3332
- R. Adam, M. Arnaud, I. Bartalucci et al. (2017), A&A 606, A64, arXiv:1706.10230  
Mapping the hot gas temperature in galaxy clusters using X-ray and Sunyaev-Zel'dovich imaging
- F. Ruppin, R. Adam, B. Comis et al. (2017), A&A 597, A110, arXiv:1607.07679  
Non parametric deprojection of NIKA SZ observations: pressure distribution in the Planck-discovered cluster PSZ1 G045.85+57.71
- R. Adam, I. Bartalucci, G. W. Pratt et al. (2017), A&A 598, A115, arXiv:1606.07721  
Mapping the kinetic Sunyaev-Zel'dovich effect toward MACS~J0717.5+3745 with NIKA
- R. Adam, B. Comis, I. Bartalucci et al. (2016), A&A 586, A122, arXiv:1510.06674  
High angular resolution Sunyaev-Zel'dovich observations of MACS J1423.8+2404 with NIKA: multi-wavelength analysis
- R. Adam (2015), Ph.D. thesis, <https://tel.archives-ouvertes.fr/tel-01303736> (in French)  
Observation des amas de galaxies par effet Sunyaev-Zel'dovich et de la polarisation du fond diffus cosmologique : de Planck à NIKA
- R. Adam, B. Comis, J. F. Macías-Pérez et al. (2015), A&A 576, A12, arXiv:1410.2808  
Pressure distribution of the high-redshift cluster of galaxies CL J1226.9+3332 with NIKA
- A. Catalano, M. Calvo, N. Ponthieu, R. Adam et al. (2014), A&A 569, A9, arXiv:1402.0260  
Performance and calibration of the NIKA camera at the IRAM 30m telescope
- R. Adam, B. Comis, J. F. Macías-Pérez et al. (2014), A&A 569, A66, arXiv:1310.6237  
First observation of the thermal Sunyaev-Zel'dovich effect with kinetic inductance detectors

## Contact and external links:

### Email:

Remi.Adam@oca.eu  
radam@cefca.es

### Useful links:

NIKA2 website: <http://ipag.osug.fr/nika2/Welcome.html>  
NIKA2 wiki: <http://www.iram.es/IRAMES/mainWiki/NIKA/Main>  
NIKA2 projects <http://lpsc.in2p3.fr/NIKA2Sky/>  
IRAM website: <http://www.iram-institute.org/>